The Plant Cell, Vol. 7, 2115–2127, December 1995

Molecular Characterization of the *CER1* Gene of Arabidopsis Involved in Epicuticular Wax Biosynthesis and Pollen Fertility

Mark G. M. Aarts,[a] Christian J. Keijzer,[b] Willem J. Stiekema,[a] and Andy Pereira[a,1]

[a] Department of Molecular Biology, Dienst Landbouwkundig Onderzoek–Centre for Plant Breeding and Reproduction Research, Postbus 16, 6700 AA Wageningen, The Netherlands

[b] Department of Plant Cytology and Morphology, Wageningen Agricultural University, Arboretumlaan 4, 6703 BD Wageningen, The Netherlands

The aerial parts of plants are coated with an epicuticular wax layer, which is important as a first line of defense against external influences. In Arabidopsis, the *ECERIFERUM* (*CER*) genes effect different steps of the wax biosynthesis pathway. In this article, we describe the isolation of the *CER1* gene, which encodes a novel protein involved in the conversion of long chain aldehydes to alkanes, a key step in wax biosynthesis. *CER1* was cloned after gene tagging with the heterologous maize transposable element system *Enhancer-Inhibitor*, also known as *Suppressor-mutator*. *cer1* mutants display glossy green stems and fruits and are conditionally male sterile. The similarity of the CER1 protein with a group of integral membrane enzymes, which process highly hydrophobic molecules, points to a function of the CER1 protein as a decarbonylase.

INTRODUCTION

Waxes are found in a wide variety of living organisms as a mixture of long chain fatty acid–derived substances (Kolattukudy, 1976). In plants, these components are specifically found as an epicuticular layer that covers leaves and young stems and is often visualized by a characteristic glaucous appearance (Kolattukudy, 1975). The primary function of epicuticular wax deposition is to reduce water loss through the epidermis (Hall and Jones, 1961), a feature contributing to drought tolerance. In addition, this outer layer has a major function in the interaction with herbivorous insects and plant pathogenic fungi (Thompson, 1963; Städler, 1986; Podila et al., 1993; Eigenbrode and Espelie, 1995). An unexpected function of wax has been described recently by Preuss et al. (1993), who found pollen wax composition and structure to be important factors for a proper pollen–pistil interaction.

The wax composition is determined by the various biochemical steps of wax biosynthesis. Plant wax layer mutants, which unravel these biochemical steps, are available (von Wettstein-Knowles, 1979; Kolattukudy, 1980; Bianchi et al., 1985) and have led to a basic outline of the wax biosynthetic pathway (von Wettstein-Knowles, 1979; Bianchi et al., 1985; Lemieux et al., 1994; von Wettstein-Knowles, 1994). Starting with hexadecanoic acid, long chain fatty acids with an even carbon number (in general, C_{20} to C_{32}) are produced by elongation. These fatty acids are reduced to fatty aldehydes and primary alcohols or reduced and decarbonylated to yield alkanes with an uneven carbon number (Cheesbrough and Kolattukudy, 1984). The latter can be further converted to secondary alcohols and ketones (Kolattukudy, 1980).

Many genetic loci influencing wax deposition have been identified in maize, barley, *Brassica* spp, and Arabidopsis (Baker, 1974; von Wettstein-Knowles, 1979; Bianchi et al., 1985; Koornneef et al., 1989; McNevin et al., 1993). Mutants with altered wax production or wax composition are in general characterized by a bright green phenotype. In Arabidopsis, there is an additional effect on fertility for some mutants, and the 21 different genetic wax layer or *ECERIFERUM* (*CER*) loci identified in Arabidopsis have been grouped into four classes based on fertility and visual degree of glossiness of the mutants (Koornneef et al., 1989; McNevin et al., 1993). Isolation of these *cer* genes will contribute to the understanding of pollen–pistil interactions as well as plant–herbivorous insect interactions. Furthermore, it may provide tools for the manipulation of wax composition in crop species to generate a source of broad host range resistance against herbivorous insects. A highly active transposon tagging system based on the autonomous *Enhancer* or *Suppressor-mutator* (*En/Spm*) and nonautonomous *Inhibitor* or *defective Suppressor-mutator* (*I/dSpm*) elements from maize has been developed in our laboratory for Arabidopsis (Aarts et al., 1993, 1995), and we used it to generate transposon-mutagenized populations that were screened for *cer* mutants.

In this article, we report the identification and phenotypic analysis of an *I/dSpm* transposon-tagged *cer1* mutant and the

[1] To whom correspondence should be addressed.

subsequent isolation and characterization of the *CER1* gene involved in wax biosynthesis and pollen fertility. Stem wax of *cer1* mutants has been analyzed previously (Hannoufa et al., 1993; McNevin et al., 1993; Lemieux et al., 1994) and found to be especially rich in aldehydes but lacking alkanes, suggesting that the CER1 protein is involved in the conversion of aldehydes to alkanes. We present evidence for the function of the CER1 protein as an aldehyde decarbonylase.

RESULTS

Phenotypic and Genetic Analysis of a Transposon-Induced *cer* Mutant

To isolate genes involved in epicuticular wax biosynthesis, we used an *IldSpm* transposon tagging approach to generate and screen Arabidopsis lines containing the *En/Spm–IldSpm* transposon tagging system (see Methods; Aarts et al., 1995). Among the screened lines, we selected one line with multiple *IldSpm* elements and the TEn2 transposase T-DNA (Aarts et al., 1995), which revealed some bright green semisterile mutants among normal wild-type plants. Phenotypically, these mutants strongly resemble a known class of *cer* mutants with a glossy stem and reduced fertility (Koornneef et al., 1989). Complementation tests with the *cer1*, *cer3*, *cer6*, and *cer10* mutants in this class revealed that the transposon-induced mutant is allelic to *cer1-1*. No clear phenotypic differences were found between our *cer1* mutants (which we called *cer1-m*) and *cer1-1* mutants. Both display a strong glossy stem and fruit phenotype, without any visible sign of wax production. Wax production on other organs of the plant was apparently not altered, but epicuticular wax production in wild-type plants is mainly confined to stem and fruit surface and not visually detectable on other parts of the plant.

Mutation of *cer1* not only alters the wax deposition on stem and fruit but also has a pleiotropic effect on plant fertility. A similar effect has been observed for *cer6-2* or *pop1* (defective in pollen–pistil interactions), described as a conditionally male-sterile *cer* mutant, but was never characterized for *cer1* mutants; therefore, we decided to examine the cause of sterility in much the same way as was performed for *cer6-2* (Preuss et al., 1993). Although normal amounts of pollen are produced by the *cer1-1* and *cer1-m* mutants, they were completely self-sterile under dry conditions (30 to 40% relative humidity). Crossing *cer1-m* mutant flowers with wild-type Landsberg *erecta* pollen led to a normal seed set. Self-fertility was increased to the wild-type level by growing the plants under high humidity (90 to 100% relative humidity), indicating that, as with *cer6*, the self-sterility is an environmentally controlled form of male sterility (Preuss et al., 1993). We tested germinaton of *cer1-m* and Landsberg *erecta* wild-type pollen on mutant and wild-type stigma papillae (see Methods) and found that mutant pollen does not germinate on either wild-type or *cer1-m* pistils, whereas the pollinations with wild-type pollen were normal, yielding normal seed set. Pollen from *cer1-m* mutants germinates similarly to wild-type pollen in vitro (data not shown). The inability of *cer1-m* pollen grains to germinate in vivo coincided with the inability to rehydrate on the stigma surface, as was also reported for the *cer6-2* mutant. Rehydration of wild-type pollen grains occurred within minutes after deposition on the stigma papillae, during which time the pollen grain swelled to about twice its original size (Preuss et al., 1993; M.G.M. Aarts, unpublished observations). The accumulation of callose on the stigma surface in response to pollination, which was observed for *cer6-2* pollen (Preuss et al., 1993), was also seen when fully receptive wild-type or *cer1-m* stigmae were pollinated with *cer1-m* pollen but not when pollinated with oilseed rape or petunia pollen (data not shown).

In terms of pollen–pistil interaction, the *cer1* mutants are very similar to *cer6-2* mutants. For the latter mutant, conditional male sterility is explained based on an alteration of the tryphine layer covering the pollen grain (Preuss et al., 1993). When examined in a scanning electron microscope, exines of mature, shed pollen of wild type, *cer1-m*, and *cer1-1* all appeared to contain tryphine, which generally was found covering the entire pollen grain (Figure 1A). Transmission electron microscopy indicated that the amount of lipid in the tryphine of the three genotypes examined was comparable. However, lipid droplets in the tryphine of *cer1-m* and *cer1-1* pollen (Figures 1C and 1D) were more numerous and considerably smaller than in tryphine of wild-type pollen (Figure 1B).

cer1-m Mutant Is Tagged by an *IldSpm* Element

The *cer1-m* mutant was found in a line with transposing *IldSpm* elements and was presumably caused by insertion of an *IldSpm* element. To determine whether *cer1* was tagged, large offspring populations from mutants were screened for progeny that had reverted to the wild-type phenotype. This is a phenomenon typical of transposon-induced mutations. Germinal reversions were found at a frequency between 1 in 50 and 1 in 300 in four independent progenies, indicating that the unstable mutation was indeed due to a transposon insertion in the *CER1* gene.

DNA blot analysis of segregating progeny (see Methods) revealed one *IldSpm* insert (*IldSpm89*) cosegregating with the *cer1-m* mutant phenotype. The flanking DNA of this *IldSpm89* insert was amplified by inverse polymerase chain reaction (IPCR) and cloned. Based on the DNA sequence, primers were designed for PCR amplification of wild-type and revertant *IldSpm89* excision alleles. Three independently derived germinal revertant plants all contained an excision allele, demonstrating that the *cer1-m* mutant was indeed tagged by the *IldSpm89* insertion, creating a *cer1::IldSpm89* allele. Excision of *IldSpm* elements normally creates short base pair deletions and additions (Aarts et al., 1993), but in these three cases, the DNA sequences of the revertant alleles were iden-

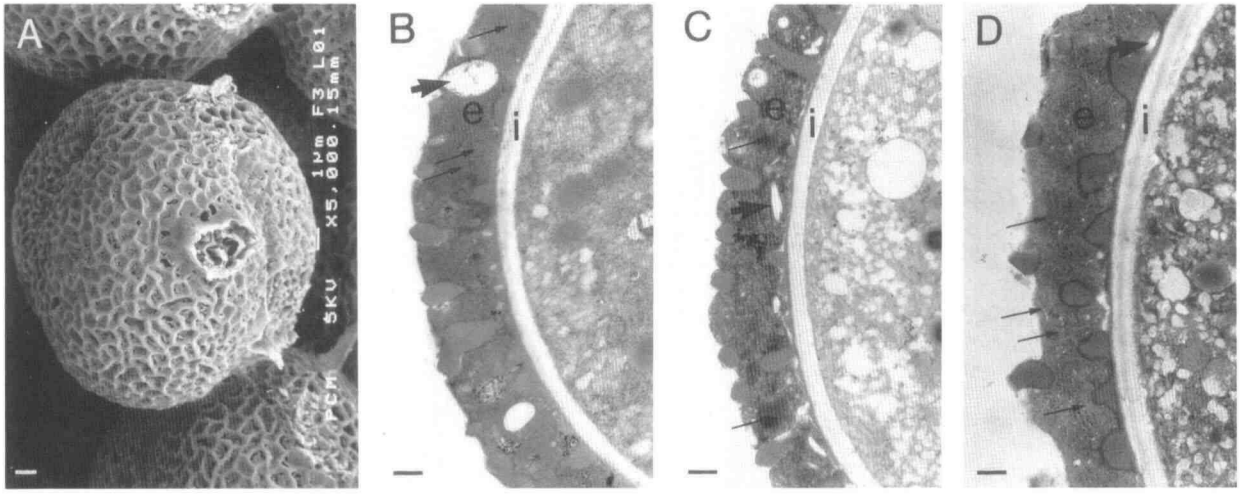

Figure 1. Tryphine on the Pollen Grains of Wild-Type Plants and *cer1-1* and *cer1-m* Mutants.

(A) Scanning electron microscopy of a *cer1-1* pollen grain with tryphine covering its entire surface. Bar = 1 μm.
(B) Transmission electron microscopy showing detail of a cross-section through a Landsberg *erecta* wild-type pollen grain. Tryphine can be observed filling the exine. Bar = 500 nm.
(C) Transmission electron microscopy showing comparable detail of a cross-section through a *cer1-1* pollen grain. Bar = 500 nm.
(D) Transmission electron microscopy showing comparable detail of a cross-section through a *cer1-m* pollen grain. Bar = 500 nm.
Tryphine in *cer1-1* and *cer1-m* appears more granulated than in the wild type and has more but smaller lipid droplets and gas inclusions. Exine (e), intine (i), gas inclusions (thick arrows), and lipid droplets (thin arrows) are indicated in **(B)** to **(D).** Gas inclusions are the white spherical or irregularly shaped spaces within the exine cavities. Lipid droplets are spherical or oval-shaped gray inclusions in the exine, which do not contrast very well with the rest of the tryphine but can be distinguished due to the amorphous structure of their contents.

tical to the wild-type DNA sequence, suggesting insertion of *IldSpm89* at a vital position of the gene.

The availability of a transposon-tagged *cer1* mutant allowed an easy screen for determining whether the *CER1* gene acts cell autonomously. The presence of clearly cell-specific somatic reversion sectors would mean a cell-autonomous expression. Somatic reversions were observed on the stem of ~20% of the mutant plants. Such variegated plants showed one or more very small glaucous gray sectors of wax deposition on a bright green background (Figure 2A). The distinct boundaries of the wild-type revertant sectors on the stem suggested a cell-autonomous expression of *CER1*. Scanning electron micrographs of these sectors revealed individual epidermal cells with overlaying wax deposition shown as the rodlike wax structures typical for Arabidopsis (Figure 2B; Koornneef et al., 1989). At higher magnification, it was clear that the effect of reversion was not completely cell autonomous, because some wax structures had formed on epidermal cells flanking revertant cells (Figure 2C). Either the *CER1* gene product or the wax components generated by this gene product had diffused a short distance away from the producing cell.

The TEn2 *En*-transposase, present in the *cer1-m* mutants, induces in general a low frequency of transposition, and therefore, we combined the *cer1*::*IldSpm89* allele with TEn5, a different, more active *En/Spm* transposase locus (Aarts et al., 1995; see Methods), which increased approximately fivefold the number of variegated mutants and the size and number of wild-type sectors per plant. To determine the effect of *CER1* expression in different layers, we searched for large excision sectors that extended over whole inflorescences. One such sector was found, and to our surprise, this sector now had wild-type stem wax and displayed a concomitant reversion to wild-type fertility. To test whether the reversion had occurred in the L2 layer, 22 offspring descending from the reverted inflorescence were sown. All offspring were found to be *cer1* mutants, suggesting that the excision was L1 rather than L2 layer specific.

Cloning of *CER1*

Using the *IldSpm89* flanking genomic DNA as a probe, a homologous cDNA clone and a 17-kb genomic clone were isolated from the respective DNA libraries. To confirm that the cDNA clone originated from the *CER1* locus, part of the insert DNA was used as a probe and hybridized to a blot of *cer1*::*IldSpm89* mutant and revertant plants (Figure 3). All mutants were homozygous for a fragment containing the *IldSpm89* insert,

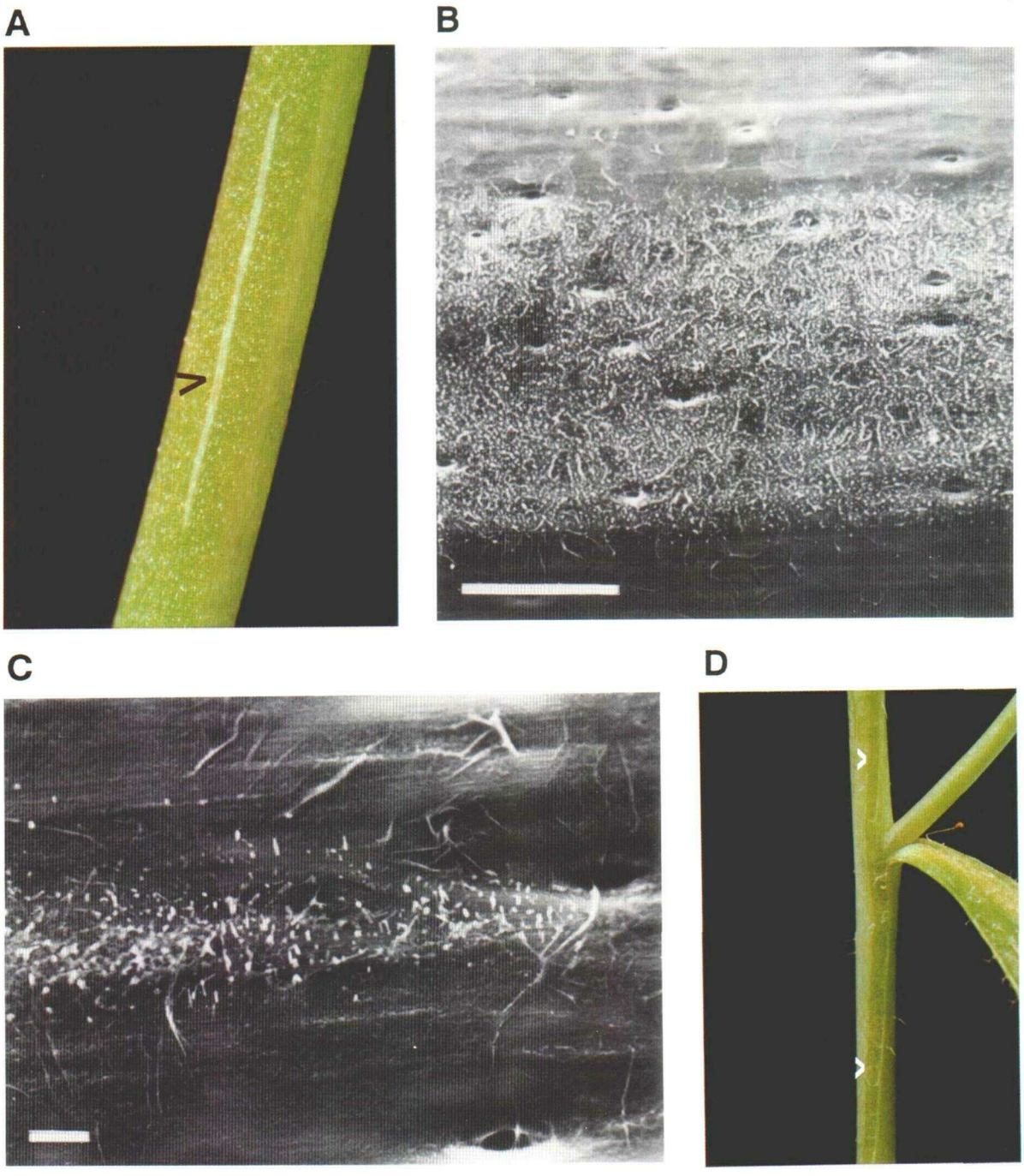

Figure 2. Phenotype of a Transposon-Tagged *cer1* Mutant.

(A) Bright green stem of a *cer1*::*IldSpm* mutant. The black arrowhead indicates a glaucous wild-type somatic excision sector.
(B) Scanning electron microscopy of a wild-type excision sector similar to the one shown in **(A).** Bar = 100 μm.
(C) One-cell-wide excision sector with wild-type epicuticular wax production. The presence of the typical wild-type Arabidopsis epicuticular wax rods is not limited to the surface directly above the epidermal cells carrying the excision, but some wax structures are formed on neighboring cells. Bar = 10 μm.
(D) Stem of a wild-type (*CER1cer1*::*IldSpm89*) plant with a *cer1* mutant sector (white arrowheads).

although excision could be observed, and all revertants were either hemizygous for the *I/dSpm89* insert or lacked the insert.

Conclusive proof that the isolated gene was indeed the *CER1* gene involved in epicuticular wax formation was obtained from the analysis of a plant with wild-type phenotype except for a small mutant *cer* sector (Figure 2D). In the course of *cer1*::*I/dSpm89* analysis, three such plants were found in various progeny. The mutant sector in one of these plants, hemizygous for *I/dSpm89*, ended in a small leaf, from which DNA was isolated for PCR analysis. Combinations of an *I/dSpm*-specific terminal primer and different *CER1*-specific primers (see Methods) were used for PCRs with DNA from the *cer* sector and from the wild-type rosette leaves of the same plant (Figure 4A). Two *cer* sector–specific DNA fragments were amplified for two primer combinations. The new *cer* sector–specific *I/dSpm* insertion was positioned within the coding region of the cloned gene, 1.0 kb upstream of the *I/dSpm89* insert (Figure 4B). Because a new insertion of an *I/dSpm* element into the cloned gene resulted again in a mutant *cer* phenotype, we conclude that the cloned gene is indeed *CER1* involved in epicuticular wax biosynthesis.

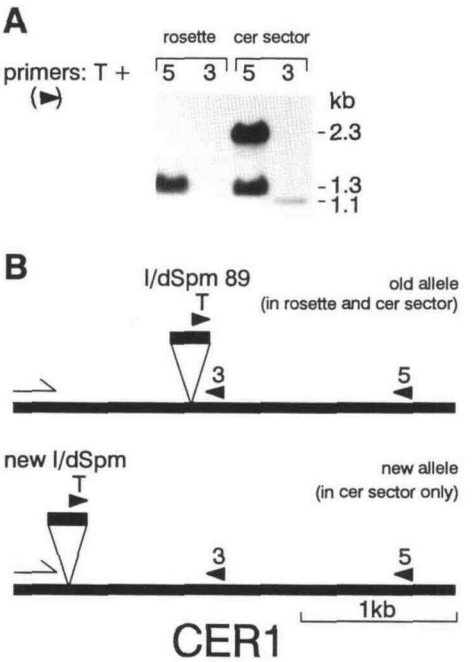

Figure 4. A *cer* Mutant Sector on a Wild-Type *CER1cer1*::*I/dSpm89* Plant Is Caused by a New Insertion of an *I/dSpm* Element in the *CER1* Gene.

(A) Gel blot hybridization of the *CER1* cDNA probe to DNA from four PCRs performed with primer combinations T and 5, and T and 3 on DNA from rosette leaves (rosette) or from a cauline leaf on which a *cer* sector (cer) (see Figure 2D) ended. Primer T is a terminal inverted repeat primer specific to *I/dSpm* elements, and primers 3 and 5 are specific to the *CER1* gene, with their hybridization sites 1.2 kb apart. DNA polymerase extends from these primers toward the 5′ end of the gene. With rosette and cer DNA, the combination of primers T and 5 amplified a 1.3-kb fragment derived from the *cer1*::*I/dSpm89* (old) allele. Only with cer DNA, the same primer combination amplified an extra 2.3-kb fragment derived from a new mutant *cer1* allele, replacing the wild-type rosette *CER1* allele by insertion of another *I/dSpm* element. This new allele was confirmed with the primer combination T and 3, which amplified a 1.1-kb fragment only with cer DNA. The expected common fragment of 0.1 kb derived from the *I/dSpm89* insertion was too small to be seen on the DNA gel blot.

(B) Schematic representation of the position of the primers (arrowheads) used in **(A)** and of the insertions of *I/dSpm89* (old) and another *I/dSpm* element (new) in the *CER1* gene. The old allele is present in both the rosette and cer samples, and the new allele specific to the cer sample has replaced the wild-type *CER1* allele present in the rosette sample. The arrows indicate the direction of the *CER1* reading frame.

Analysis of the *CER1* cDNA

Epicuticular waxes are found mainly on the stem and fruit epidermis of Arabidopsis, and the isolated *CER1* gene should be expressed in these organs. *CER1* transcription was therefore tested by RNA gel blot hybridization, and as expected, the *CER1* transcript was found in wild-type stem and fruit tissue. Additional strong expression was detected in Arabidopsis flowers, in which expression of the *CER1* gene could be expected based on the male-sterile phenotype of the mutant. Arabidopsis has little wax formation on the leaves, explaining the low level of leaf transcript (Figure 5A). Transcription of the *CER1* gene was blocked in *cer1*::*I/dSpm89* mutant flowers, whereas transcription in *cer1-1* flowers was not affected (Figure

Figure 3. All Wild-Type Revertant Offspring of a Homozygous *cer1*::*I/dSpm89* Mutant Have at Least One *CER1* Excision Allele.

EcoRI-digested DNAs of the *cer1*::*I/dSpm* parental plant, the wild-type revertant, and *cer1* mutant offspring were probed with part of the *CER1* cDNA. The 9.8-kb EcoRI fragment present in the parental plant represents the *cer1*::*I/dSpm89* allele with the transposon insert. Excision of the 2.2-kb *I/dSpm89* element results in a 7.6-kb *CER1* allele EcoRI fragment, which is present in all revertants. All mutants show somatic excision of *I/dSpm89* from their two *cer1*::*I/dSpm89* insertion alleles leading to a small amount of the 7.6-kb EcoRI excision fragment in these lanes.

5C). The mutant phenotype of the chemically induced *cer1-1* mutant is probably due to a minor rearrangement such as a point mutation. In flowers of the F_1 hybrid between *cer1::IIdSpm* and *cer1-1*, the transcription level of the gene was the intermediate of the two parents (Figure 5C).

The 2109-bp *CER1* cDNA contains an open reading frame of 625 amino acids (Figure 6A). Part of the corresponding genomic DNA sequence was determined, and an in frame stop codon was found 33 bp upstream of the ATG start codon, indicating that the cDNA clone comprises the complete open reading frame. A putative TATA transcription initiation sequence is present 72 bp upstream of the ATG start codon in the genomic DNA sequence. The predicted protein has an apparent molecular mass of 72.3 kD and a pI of 8.23. Analysis of the amino acid sequence with the PC/Gene computer package classifies the protein as an integral membrane protein. Two putative transmembrane helices are predicted, stretching from amino acid positions 178 to 213 and 325 to 350 (Figure 6A), and additional membrane-associated helices cover amino acid positions 7 to 27, 45 to 65, 99 to 119, and 126 to 146. Two possible Asn glycosylation sites are found at positions 258 and 456. Insertion of *IIdSpm89* disrupts the reading frame from Thr (amino acid position 272) onward (Figure 6A).

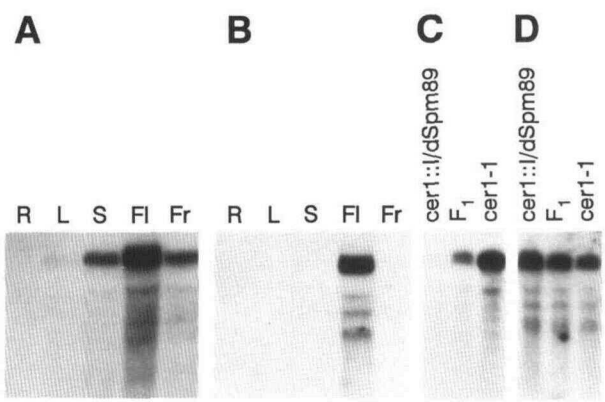

Figure 5. Transcription of the *CER1* and *CER1*-like Genes in Arabidopsis.

(A) RNA gel blot of 10 μg of root (R), leaf (L), stem (S), flower (Fl), and fruit (Fr) total RNA, hybridized with the 822-bp 3′ part of the *CER1* cDNA. There is no transcription in root, little in leaf, and strong transcription in stem, flower, and fruit.

(B) Duplicate RNA gel blot of **(A)**, hybridized with the ATTS1001 (EST) insert *CER1*-like probe, detects strong transcription in flower tissue only. The detected RNA is of a length similar to that in **(A)**.

(C) RNA gel blot of total flower RNA from *cer1::IIdSpm89*, an F_1 between *cer1::IIdSpm89* and the chemically induced *cer1-1* mutant, and the *cer1-1* parent, hybridized with the *CER1* probe used in **(A)**. *CER1* transcription is almost completely blocked by the homozygous *IIdSpm89* insertion but only half blocked in the hemizygote and not at all blocked in the chemically induced *cer1-1* mutant.

(D) Same RNA gel blot as shown in **(C)**, stripped and rehybridized with the *CER1*-like probe used in **(B)**. There is no difference in transcription between the three tested plants, showing that transcription of the *CER1*-like gene is in no way affected by transcription of the *CER1* gene.

CER1 Homologs Are Present in Other Species

Wax production is common to many plant species, and genes involved in wax biosynthesis may well be conserved among species. This was confirmed as data base searches, performed with the *CER1* cDNA and predicted amino acid sequences, revealed significant homologies with cDNA and expressed sequence tag (EST) sequences from both dicot and monocot species (see Methods). The predicted amino acid sequence of the EST ATTS1001 cDNA isolated from flower buds of Arabidopsis showed 53.8% identity with the C-terminal region (210 amino acids) of the predicted *CER1* amino acid sequence (Figure 6A). In addition, a *B. campestris* flower bud EST was found with 49.1% predicted amino acid sequence identity (117 amino acids), a potato epidermal EST with 67.4% amino acid identity (46 amino acids), and a *Senecio odorus* epidermal cDNA with 31.3% amino acid identity (513 amino acids) (Figure 6A).

This family of related sequences could be extended to the monocot species maize and rice. A maize vegetative meristem EST showed 52.7% amino acid identity over 110 amino acids. The homology of two rice callus cDNAs sequenced from their 5′ end started exactly at the N terminus of the predicted *CER1* amino acid sequence extending over the entire length of sequenced cDNA, representing ~80 amino acids (37.5% overall identity; Figure 6B). Interestingly, the predicted amino acid sequence of another rice cDNA with a short stretch of amino acid similarity with the predicted *CER1* amino acid sequence showed additional homology in this region with the C-5 sterol desaturase protein of yeast encoded by the *ERG3* gene (Arthington et al., 1991). These two short stretches of homology are conserved among CER1, SOLIPTRB, rice EST D23996, and ERG3, and a part of it is also found in maize EST T70657 (Figure 7). Each stretch of homology reveals a short motif with the consensus sequence Tyr-His-Ser/Thr-X-His-His (where X stands for any amino acid).

A *CER1*-like Gene Is Closely Linked to the *CER1* Gene but Transcribed Differently

Part of the genomic sequence upstream of the *CER1* gene was determined, and when used in a DNA data base search, DNA sequences between 1.0 and 1.7 kb upstream of the *CER1* start codon surprisingly were found to be identical with the ATTS1001 EST sequence (data not shown). The DNA sequence of ATTS1001 shows only 62.2% identity with the *CER1* cDNA (compared with the 53.8% amino acid identity found previously), and when used as a probe, it does not cross-hybridize to the *CER1* cDNA sequence. From these data, we conclude

A

```
CER1      1 MATKPGVLTDWPWTPLGSFKYIVIAPWAVHSTYRFVTDDP   40
SOLIPT    1                                  ...GDD    3

CER1     41 EKRDLGYFLVFPFLLFRILHNQVWISLSRYYTSSGKRRIV   80
SOLIPT    4 DLANNWCFHILVISLLRFNLYMWYTNICNMLFLTRNRRIL   43

CER1     81 DKGIDFNQVDRETNWDDQILFNGVLFYIGINLLPEAK-QL  119
SOLIPT   44 HQSIDFNQIDKEWNWDNFVILQALIASLAIYHFPQEFANL   83

CER1    120 PWWRTDGVLMAALIHTGPVEFLYYWLHKALHHHFLYSRYH  159
SOLIPT   84 PVWKTKGLVAIVVIHVVVSEPLYYWLHRLLHTNYLFTPYH  123

CER1    160 SHHHSSIVTEPITSVIHPFAEHIAYFILFAIPLLTTLLTK  199
SOLIPT  124 SFHHSSAVPQPVTVGSTTFLEELLVTAVLGLPILGCSLSG  163

CER1    200 TASIISFAGYIIYIDFMNNMGHCNFELIPKRLFHLFPPLK  239
SOLIPT  164 YGSKSIIYGYVLVFDFLRCLGHSNVEIMPHWIFDYFPFFR  203
                        *                  ↓
CER1    240 FLCYTPSYHSLHHTQFRTNYSLFMPLYDYIYGTMDESTDT  279
SOLIPT  205 FIIYTPTYYSLHHSEMKSNYCLFMPLYDTMWNTLNTKSWG  243

CER1    280 LYEK-TLERGDD-RVDVVH-LTHLTTPESIYHLRIGLASP  316
SOLIPT  244 LHKKISLDSGKSTRVPDFVFLAHVVDITSALHVPFVIRSF  283

CER1    317 ASYPFAYRWFMRLLWPFTSLSMIFTLFYARLFVAERNSFN  356
SOLIPT  284 SAMAYSARLFLLPLWPFTFAVMIVMWARSKTFLLSSYNLR  323

CER1    357 KLNLQSWVIPRYNLQYLLKWRKEAINNMIEKAILEADKKG  396
SOLIPT  324 GRLHQTWVVPRFGFQYFLPFACQGINNHIEEAILRADKLG  363

CER1    397 VKVLSLGLMNQGEELNRNGEVYIHNHPDMKVRLVDGSRLA  436
SOLIPT  364 VKVISLAALNKNESLNRGGTLFVKKHPNLKVRVVHGNTLT  403
AT1001    1           ...LNGSGEMYVQKYPKLKIRLVDGSSMA   26
                        *
CER1    437 AAVVINSVPKATTSVVMTGNLTKVAYTIASALCQRGVQVS  476
SOLIPT  404 AAVILNEINEDVKEVFLTGATSKLGRAIALYLCRRGVHVL  443
AT1001   27 ATVVINNIPKEATEIVFRGNLTKVASAVVFALCQKGVKVV   66

CER1    477 TLRL--DEYEKIRSCVPQECRDHLVYLTSE-ALSSNKVWL  513
SOLIPT  445 MLTLSTERFQNIQEEAPSKCRKNLVQVTKYQAAKNCKTWV  483
AT1001   67 VLRE--EEHSKLIKSGVD---KNLVLSTSN-SYYSPKVWL  100

CER1    514 VGEGTTREEQEKATKGTLFIPFSQFPLKQLRSDCIYHTTP  553
SOLIPT  484 IGKWITPGQQRWAPSGTHFHQFVVPPILAFRRTAPTETLP  523
AT1001  101 VGDGIENEEQMKAKEGTLFVPFSHFPPNKLRKDCFYQSTP  138

CER1    554 ALIVPKSLVNVHSCENWLPRKAMSATRVAGILHALEGWET  593
SOLIPT  524 L
AT1001  139 AMRVPKSAQNIDSCENWLGRRVMSAWKIGGIVHALEGWEE  178

CER1    594 HECGTSLLLSDLDKVWEACLSHGFQPLLLPHH         625
AT1001  179 HDCGNTCNVLRLHAIWEAALRHDFQPLPPSPL          210
```

B

```
CER1      1 MATKPGVLTDWPWTPLGSFKYIVIAPWAVHSTYRFVTDDP   40
D15324    1 MASKPGPLTQWPWHNLGNYKYALVAPSAAYSTYRFVTASS   40
D22308    1 MATRPGPLTEWPWHRLGNFKYVVMAPVVAHGARRVMRNGW   40

CER1     41 E-KRDLGYFLVPPFLLFRILHNQVWISLSRYYTSSGKRRIV   80
D15324   41 AAERDLLNFMVFPMLLLRLLYGQLWITVSRHQTARSKHKIV   81
D22308   41 G-DLDIAFSLILPSLLLRMIHNQIWISLSRYQTARSKHRIV   80
```

Figure 6. *CER1* Deduced Amino Acid Sequence and Comparison with Homologous Amino Acid Sequences.

(A) Amino acid sequence deduced from the *CER1* cDNA (CER1), compared with the homologous amino acid sequences derived from the partial cDNA sequence of SOLIPTRB (SOLIPT) from *Senecio odorus* and ATTS1001 (AT1001) from Arabidopsis. Two putative membrane-spanning sequences in the CER1 amino acid sequence are overlined. A histidine-rich motif is underlined. Putative glycosylated asparagine residues in the CER1 amino acid sequence are indicated (*) as well as the site of the target site duplication caused by insertion of *ldSpm89* (↓) that disrupts the reading frame in *cer1*::*ldSpm89* mutants. Dots indicate that the SOLIPTRB and ATTS1001 cDNAs are partial and that the N-terminal ends of the complete amino acid sequences are missing. **(B)** N-terminal stretch of ~80 amino acids with 37.5% identity overall between the CER1 protein and two amino acid sequences deduced from two rice cDNA clones (D15324 and D22308). Shaded boxes indicate similar amino acid residues; identical amino acid residues are indicated in boldface. Similar residues are grouped as follows: (V,L,I,M), (S,T), (Q,N,E,D), (K,R), (G,A), and (F,W,Y).

that the ATTS1001 EST clone is part of a transcribed *CER1* homologous *CER1*-like gene located directly 5′ to *CER1* and oriented in the same direction.

To confirm that this gene is transcribed in Arabidopsis and to examine any correlation between *CER1* and *CER1*-like expression, we tested *CER1*-like transcription by RNA blot hybridization using the ATTS1001 EST insert probe (Figures 5B and 5D). In contrast to the strong transcription of *CER1* in stem, flower, and fruit, transcription of the *CER1*-like gene was restricted to flowers but with a similar mRNA size and transcription level as the *CER1* gene (Figure 5B). Transcription of the *CER1*-like gene was not affected by the *cer1* mutation, as seen by the similar level of *CER1*-like transcription in the flowers of *cer1*::*ldSpm89*, *cer1-1*, and the F_1 (Figure 5D), demonstrating the difference in transcriptional regulation between *CER1* and *CER1*-like. The transcription of both the *CER1* and *CER1*-like gene in chemically or radiation-induced *cer2* to *cer9* flowers and stems was the same as in the wild type (data not shown), suggesting that none of these loci is a transcriptional regulator.

DISCUSSION

CER1 Protein Has a Function in Wax Alkane Biosynthesis

We have cloned and characterized the *CER1* gene from Arabidopsis involved in epicuticular wax biosynthesis and pollen fertility. *CER1* is a cell autonomously expressed gene, mainly active in stem, flower, and fruit and at a low level in leaf. The *cer1* mutant is one among four of the *cer* mutants with a drastically changed epicuticular wax phenotype, for which a biochemical function has been proposed to the corresponding wild-type gene. *CER2* and *CER6* are thought to encode components of fatty acid elongation, and *CER4* is suggested to be involved in fatty aldehyde reduction (Hannoufa et al., 1993; Lemieux et al., 1994; Jenks et al., 1995). Biochemical studies (Hannoufa et al., 1993; McNevin et al., 1993; Lemieux et al., 1994) have shown that *cer1* mutants are blocked in the conversion of stem wax C_{30} aldehydes (triacontanal) to C_{29} alkanes (nonacosane) and that they also lack the secondary alcohols (14- and 15-nonacosanol) and ketones (15-nonacosanone) derived thereof. Alkanes, secondary alcohols, and

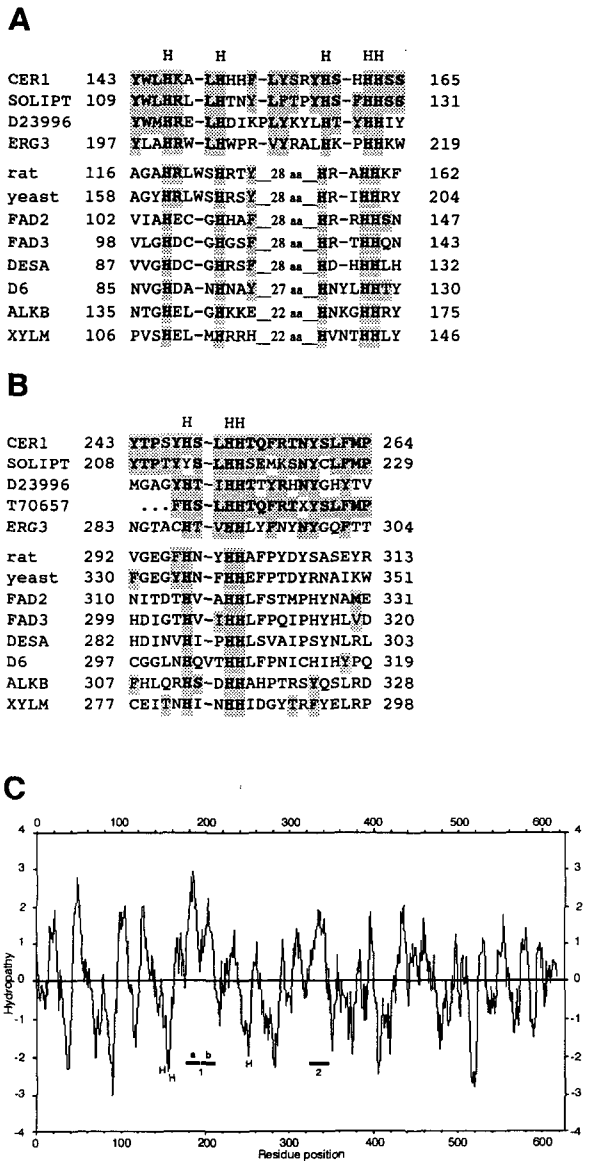

Figure 7. Comparison of the Histidine-Rich Regions from the CER1 and Other Amino Acid Sequences.

(A) Comparison of the first and second histidine-rich motifs $HX_{3-4}H$ and $HX_{2-3}HH$ (X stands for any amino acid) present in CER1 homologous sequences found after searching the sequence data bases with TBLASTN (top) and motifs present in a number of membrane-bound fatty acid desaturases, an alkane hydroxylase, and a xylene monooxygenase (bottom; Shanklin et al., 1994). The CER1 homologous sequences are derived from the SOLIPTRB (SOLIPT) cDNA from *S. odorus*, a rice EST (D23996), and the *ERG3* gene from yeast, encoding sterol C-5 desaturase. The additional integral membrane sequences shown are the stearoyl-CoA desaturase from rat (rat; Thiede et al., 1986) and yeast (yeast; Stukey et al., 1990), the Δ12 and Δ9 fatty acid desaturases from Arabidopsis (FAD2 and FAD3; Okuley et al., 1994; Arondel et al., 1992), the Δ12 fatty acid desaturase from *Synechocystis* (DESA; Wada et al., 1990), the Δ6 fatty acid desaturase from *Synechocystis* (D6; Reddy et al., 1993), the alkane hydroxylase from *Pseudomonas oleovorans* (ALKB; Kok et al., 1989), and the xylene monooxygenase from *P. putida* (XYLM; Suzuki et al., 1991). Similar and identical residues are as indicated in Figure 6.

(B) Comparison of the third histidine-rich motif $HX_{2-3}HH$ present in the same sequences as in **(A)**. The amino acid sequence derived from a partially sequenced EST clone from maize (T70657) started between the second and third histidine-rich motif and shows further homology with CER1. The second and third histidine-rich motifs are separated by a transmembrane sequence crossing the membrane twice.

(C) Hydrophobicity plot of the predicted CER1 amino acid sequence according to Kyte and Doolittle (Devereux et al., 1984), indicating the location of putative transmembrane sequences (horizontal bars labeled 1 and 2) and the histidine-rich motifs (H). Transmembrane sequence 1 is long enough to span the membrane twice (a and b).

ketones constitute ~65% of the total wax in wild-type Landsberg *erecta* (Lemieux et al., 1994). The conversion of aldehydes to alkanes is moderated by aldehyde decarbonylases (Cheesbrough and Kolattukudy, 1984), and the CER1 protein may be an enzymatic component in this biochemical step to produce long chain alkanes.

CER1 Protein Contains an Iron Binding Motif

Because no genes encoding fatty aldehyde decarbonylases have been cloned previously, this biochemical function has not been described at the sequence level. The homologies we observed between *CER1* and other cDNA or EST sequences in the sequence data bases describe a family of related proteins, but they are not very useful in defining a biochemical function for these proteins. The *S. odorus* and potato partial cDNA sequences encoding CER1 homologous amino acid sequences are described as epidermis specific, which corresponds to a function for CER1 in epicuticular wax biosynthesis. The only homology we found with a functional protein is with the C-5 sterol desaturase from yeast. This homology is actually confined to a very short sequence, centered around three histidine-rich motifs ordered as $HX_3H + HX_2HH + HX_2HH$ (where X stands for any amino acid). These, or the related $HX_{3-4}H + HX_{2-3}HH + HX_{2-3}HH$ motifs, were recently found to be conserved among a number of integral membrane fatty acid desaturases from mammals, fungi, insects, higher plants, and cyanobacteria as well as bacterial membrane alkane hydroxylase and xylene monooxygenase (Figures 7A and 7B). All eight conserved histidine residues are essential for the enzymatic function, as was tested with complementation studies in yeast using site-specific mutagenized rat stearoyl-CoA desaturase genes (Shanklin et al., 1994).

Apart from the histidine-rich motifs, there is no apparent homology with other regions of these proteins (Figures 7A and 7B), suggesting that the reported proteins with these motifs (including the C-5 sterol desaturase and the protein encoded

by the partial cDNA clone from rice) are likely to share some biochemical properties rather than performing the same biochemical function. The presence of closely spaced histidine residues is typical for metal binding motifs, and based on the requirement of fatty acid desaturases for iron, the histidine motifs are strongly suggested to be involved in the binding of iron ions (Okuley et al., 1994). The spacing separating the first two histidine motifs from the third motif, which is reported to be conserved among membrane desaturases and among the alkane hydroxylase and the xylene monooxygenase, is similar albeit slightly smaller in the CER1, SOLIPTRB, D23996, and ERG3 proteins (Figures 7A and 7B). This distance appears to be conserved within families of related proteins, because it is also smaller in the alkane hydroxylase and the xylene monooxygenase compared with the desaturases. One reason there is some variation in the spacing between the first two and the third histidine motifs among protein families is that the structure of this protein part, rather than the spacing between the motifs, is important for function of the proteins. All proteins with the histidine-rich motifs described so far were found to contain long hydrophobic domains between the first two and the third histidine motifs (Shanklin et al., 1994). These domains are able to span a membrane twice. The same is found for the CER1, SOLIPTRB, and ERG3 protein, in which both HX_2HH motifs are separated by a predicted transmembrane sequence that can be divided into two parts long enough to satisfy this requirement (Figure 7C).

Based on all these characteristics, the CER1 protein closely resembles a class of structurally and perhaps evolutionarily related integral membrane enzymes that share the preference for highly hydrophobic substrates, the presence of metal binding histidine-rich motifs, and the need for electron donors to perform their catalytic function.

CER1 Protein as Part of an Aldehyde Decarbonylase

The CER1 protein has been proposed to function in the decarbonylation of aldehydes to alkanes (Hannoufa et al., 1993; Lemieux et al., 1994). So far, two plant aldehyde decarbonylases (from pea and a green colonial alga, *Botryococcus braunii*) have been studied in some detail (Cheesbrough and Kolattukudy, 1984; Dennis and Kolattukudy, 1992). Both are integral membrane proteins, with the pea decarbonylase suggested to be located in the cuticular cell membrane and the alga decarbonylase in the microsomal membranes. Both use highly hydrophobic fatty aldehydes as substrate and need metal ions for their function. The metal identity is known only for the purified decarbonylase from *B. braunii*, which interacts with cobalt present in a cobalt–porphyrin or corrin structure (Dennis and Kolattukudy, 1992). The partially purified decarbonylase from pea is merely known to depend on metal ions, because the activity is severely inhibited in the presence of metal ion chelators (Cheesbrough and Kolattukudy, 1984). All enzymatic proteins with the histidine-rich motifs identified so far are proposed to have nonheme iron-containing active sites (Shanklin et al., 1994). This is in contrast with the observed interaction of *B. braunii* decarbonylase with porphyric cobalt, but to assume all plant decarbonylases interact with heme-bound metals based on the characterization of only one (lower) plant decarbonylase would be a bit premature. It can still be envisaged that decarbonylases from higher plants use nonheme iron rather than heme cobalt. The observed biochemical properties of the partially purified aldehyde decarbonylase from pea (an integral membrane protein processing highly hydrophobic molecules in the presence of metal ions) underpin the properties ascribed to the CER1 protein on the basis of homology with some functional integral membrane enzymes. This is strong supporting evidence for the CER1 protein acting as the catalytic iron-containing part of a fatty aldehyde decarbonylase enzyme involved in the Arabidopsis epicuticular wax and pollen tryphine alkane biosynthesis.

The aldehyde decarbonylase from pea is thought to be present in the extracellular or cuticular matrix of the epidermis (Cheesbrough and Kolattukudy, 1984). This is also the case for certain nonspecific lipid transfer proteins suggested to be involved in cuticle formation (Sterk et al., 1991; Thoma et al., 1993; Pyee et al., 1994). In the absence of a signal sequence, the CER1 protein may be transported post-translationally to the cell membrane, where the putative membrane-spanning helices allow it to be anchored, with the histidine motifs probably located on the intracellular side. Wax biosynthesis at the site of wax deposition outside the cell can explain the diffusion in wax structures from the surface of stem epidermal cells with a functional *CER1* gene to cells without the gene, as we observed in a wax layer–variegated Arabidopsis plant (Figure 2C).

CER1 Protein Is Needed for Pollen Fertility

In addition to stem wax alkane synthesis, the *CER1* gene has an essential function in pollen development. *cer1* mutants have a stem wax and male sterility phenotype very similar to that of *cer3* and *cer6* mutants. As in *cer1* mutants, both the stem and leaf wax alkane content of *cer3* and *cer6* mutants is low (Lemieux et al., 1994; Jenks et al., 1995). For *cer6-2* mutants, the pollen lipid content has been examined biochemically and was found to be equally low in alkanes and wax components derived thereof (Preuss et al., 1993). The similarity in phenotype and the concomitant absence of stem alkanes in *cer1* and *cer6* mutants lead us to conclude that the CER1 protein performs a similar function in pollen tryphine synthesis and in stem wax synthesis. The low pollen alkane content of the *cer6-2* mutants was accompanied by the virtual absence of a tryphine layer deposited on the mature pollen grain (Preuss et al., 1993). Conditional male sterility of *cer1::IldSpm89* and *cer1-1* mutants was not linked to a reduction of the tryphine deposition on the pollen grains. Although the lipid in the tryphine of both *cer1* mutants was more dispersed than in tryphine of the wild-type pollen grains, the total amount of (visible) lipids in the tryphine

was similar for all three genotypes. As a whole, the entire tryphine consistently showed a more granular appearance in the two *cer1* mutants. This might have to do with a further state of tapetal cytoplasm degeneration before tryphine deposition. Also, the capillary process of tryphine transfer to the exine layer of pollen grains might influence the final texture of the tapetal remnants. As with both *cer1* mutants, the conditionally male sterile *cer6-1* mutant also does not show a reduction in tryphine deposition (Preuss et al., 1993; C.J. Keijzer, unpublished observations), in contrast with the *cer6-2* mutant. It must be noted that a correct observation of this phenomenon requires a strictly timed fixation: shortly before anthesis, tryphine can be found only inside the tapetal membrane sacs, and as late as a few hours before anther dehiscence, it is transferred to the exines of the pollen grains. Analyzing still closed anthers (sometimes even found in open flowers) might lead to the incorrect conclusion that pollen grains of a given plant lack tryphine.

Based on the electron microscopic analyses, pollen sterility in *cer1* mutants is clearly not a mechanistic problem associated with lack of tryphine as it might be in *cer6-2* mutants. Tryphine deposition is a passive process following degradation of tapetal cells. The differences in tryphine composition and ultrastructure must therefore be a direct consequence of differences in tapetum between the wild type and *cer1* or *cer6* mutants. Lack of tapetal *CER1* or *CER6* activity results in a different constitution of tapetal remains, and depending on the severity of tapetal alterations caused by *cer1* or *cer6* mutations, the tryphine composition and ultrastructure show less or more visible differences with wild-type tryphine. Our observations with *cer1* mutants emphasize the hypothesis proposed by Preuss et al. (1993) that long chain lipid molecules, in particular alkanes, are needed in the tryphine layer for proper pollen–pistil signaling. These lipids are produced in the tapetum, and because they are probably not needed for proper tapetal functioning, their absence will not affect tapetal appearance but is visible only as an altered tryphine ultrastructure in the *cer1* and *cer6* mutants. A secondary effect of the altered tryphine, which may be stress induced, is the accumulation of callose in stigma papillae in response to *cer1* and *cer6* pollen grains. No callose accumulation was observed when pollinating wild-type or *cer1* pistils with nonspecific oilseed rape or petunia pollen, and the response thus is not a general mechanism to prevent pollination by other species.

We used a cell layer chimera to study expression of *CER1* in flowers. One *cer1::IldSpm89* plant with a fertile revertant inflorescence sector containing phenotypically normal stem wax was found. In plant development, the reproductive cells, including the tapetum, descend from the L2 layer (Goldberg et al., 1993), and the epidermis descends from the L1 layer. We therefore tested offspring from the sector, which were all *cer1* mutants, showing that the *cer1::IldSpm89* to *CER1* reversion did not occur in the L2 layer but only in the L1 layer. Unexpectedly, *CER1* expression in the L1 layer alone was enough to restore a fertile phenotype, inferring that there is some mechanism for transporting the CER1 protein or its products to the tapetum or pollen wall.

The *CER1* Gene Is Conserved among Plant Species

Genes performing steps in such a general plant biosynthetic pathway as wax synthesis are expected to be found in many plant species. This is indeed the case for the *CER1* gene; we found homologs from a related Brassicae species, from the unrelated Compositae *S. odorus*, and from the even more distantly related monocot species rice and maize. By comparing the derived amino acid sequences, it is clear that all members of the *CER1* gene family we have found encode equally divergent homologous proteins. The level of identity among these proteins (between 30 to 70%) is in the same range as the homology found among fatty acid desaturases from different species, irrespective of the position of the double bond they introduce (Iba et al., 1993; Okuley et al., 1994; Sakamoto et al., 1994).

Based on the level of identity, the CER1 homologous proteins are presumably all performing a similar function. At least one additional *CER1* family member is present in Arabidopsis. The *CER1*-like gene, as we termed it, is physically (and genetically) linked to *CER1*, with a physical distance of only 1 kb. This *CER1* gene cluster most likely originated from an ancient gene duplication. Since then, both genes have evolved to such an extent that the ATTS1001 partial cDNA clone derived from the *CER1*-like gene is not recognized by the *CER1* cDNA probe upon DNA gel blot hybridization. Also, their expression patterns have changed. The *CER1*-like gene is transcribed only in flowers and is therefore not involved in stem wax biosynthesis. A function of the *CER1*-like gene in epicuticular wax biosynthesis on flower petals or sepals is unlikely, given the visual absence of wax structures on flower organs; this contrasts with the high expression of the *CER1*-like gene. By analogy to the range of fatty acid desaturases that use different unsaturated fatty acids as substrate, the CER1-like protein may have a function similar to that of the CER1 protein in pollen development, for instance, in the production of alkenes in tryphine. Alternatively, it may be expressed in another part of the flower. The lipid transfer protein LTP1 is known to be expressed in stigma papillae, where it can function in the secretion of stigma lipids (Thoma et al., 1994), and the CER1-like protein may be involved in the production of these lipids.

Conclusions

The isolation of *CER1* is a first step in understanding the biosynthesis of epicuticular wax components. The CER1 protein is part of an integral cell membrane enzyme that we deduce to be an aldehyde decarbonylase. The presence of histidine-rich motifs $HX_{3-4}H$ or $HX_{2-3}HH$, described as iron binding sites in fatty acid desaturases, may help to identify domains of the protein that interact with cofactors, which will provide additional knowledge of the biochemical properties of decarbonylases. The identification of *CER1* homologs allows their testing in the manipulation of wax alkane contents in other species. This can

be important for influencing drought resistance or insect resistance. For instance, in rice, drought tolerance is associated with high wax lines, especially rich in C_{29}, C_{33}, and C_{35} alkanes (O'Toole and Cruz, 1983; Haque et al., 1992), and a higher ratio of long chain to medium long chain aldehydes or alkanes promotes resistance to brown planthoppers (Woodhead and Padgham, 1988). The *CER1* gene is the first gene isolated that is responsible for pollen–pistil interaction in the self-compatible species Arabidopsis, and with it, the role of lipids in pollen–pistil signaling can be analyzed further. Meanwhile, the isolation of other wax biosynthesis genes by transposon tagging in Arabidopsis continues, providing more tools to study and modify the wax biosynthesis pathway.

METHODS

Transposon Tagging Lines and *eceriferum* Mutants

All experiments were performed with the Landsberg *erecta* ecotype of *Arabidopsis thaliana*, which was also the genetic background of the chemically or physically induced *eceriferum* (*cer*) mutants tested for phenotypic complementation (all mutants were provided by M. Koornneef, Wageningen Agricultural University). For screening, 25 transposon tagging lines of 12 plants, each with *Enhancer/Suppressor-mutator* transposase genes and nonautonomous *Inhibitor/defective Suppressor-mutator* elements that constitute the *En/Spm-I/dSpm* system, were grown individually in the greenhouse and examined for *cer* mutations. All lines were obtained after two generations of self-pollination, starting with one plant containing the TEn2 *En/Spm* transposase T-DNA locus along with several transposed *I/dSpm* elements (Aarts et al., 1995). The original *cer1::I/dSpm89* transposon–tagged mutant was found in line H12.1.6.2, containing ~15 different *I/dSpm* elements and homozygous for the TEn2 T-DNA. TEn5 is another *En/Spm* transposase line containing a different, more active T-DNA locus and no other *I/dSpm* elements. This line was crossed to a *cer1::I/dSpm89* plant, and *cer1* F_2 plants were screened for excision sectors. All plants grown for progeny were kept in Aracon containers (BetaTech, Ghent, Belgium) to prevent cross-pollination. Fertility of *cer* mutants was conditioned by keeping the plants enclosed in a plastic bag to increase relative humidity (Koornneef et al., 1989).

Identification of a *cer1-m* Cosegregating *I/dSpm* Element and Isolation of Flanking Genomic DNAs

The original *cer1-m* mutant was backcrossed to Landsberg *erecta* wild type for two generations. Genomic DNA was isolated from second backcross offspring plants and tested for the presence of *I/dSpm* elements. All plants were allowed to self, and their progeny were tested for segregation of the *cer1* phenotype to confirm linkage of an *I/dSpm* element with the *cer1* phenotype in the second backcross offspring. Genomic DNA from plants containing the *cer1*-linked *I/dSpm89* element and a few other unlinked *I/dSpm* elements was used to obtain DNA flanking both sides of *I/dSpm89* after *I/dSpm*-specific inverse PCR (IPCR; Masson et al., 1991). Additional PCR amplification using primer T (5′-GACACTCCTTAGATCTTTTCTTGTAGTG-3′), fitting both terminal inverted repeats of *I/dSpm*, enabled the isolation of fragments with minimal transposon DNA. Based on *I/dSpm89* flanking sequences, primers 2 and 3 (5′-GGAGCATGAGAATTGCAGATACC-3′ and 5′-GGCGTCGTCAGGTGAGTTAAGTGC-3′) were designed; these amplified a 189-bp wild-type DNA fragment covering the *I/dSpm89* insertion site.

cDNA and Genomic Library Screening

An amplified cDNA λ library representing different Arabidopsis tissues (Newman et al., 1994) and a Landsberg *erecta* genomic library obtained through the Arabidopsis Biological Resource Center (Ohio State University, Columbus, OH) and the European DNA Resource Centre (Max-Delbrück Laboratory, Cologne, Germany) were screened with the *I/dSpm89* IPCR fragment probe. The DNA insert of the genomic clone was subcloned as EcoRI fragments.

DNA and RNA Analysis

DNA and RNA gel blots were standardly hybridized at 65°C overnight and washed twice at 65°C with 2 × SSC (1 × SSC is 0.15 M NaCl, 0.015 M sodium citrate), 1% SDS or (more stringently) with 0.1 × SSC, 1% SDS. DNA sequences were determined using an ABI Sequencer (Applied Biosystems, Foster City, CA). *CER1* cDNA SalI and SalI-XbaI fragments were subcloned in pBluescript SK+ and sequenced. The double-stranded DNA sequence was completed using cDNA-specific primers 1 (5′-GGCCTCCGGCAATAGGTTGATG-3′), 4 (5′-GGTGCTTAGTCTGGGTCTCATG-3′), 5 (5′-CACAGGAGTGGACATTCACCAGAG-3′), and 6 (5′-CGCATGAGTGTGGCACATCCC-3′) (Isogen Bioscience, Amsterdam, The Netherlands). The same primers as well as primers 2 and 3 flanking *I/dSpm89* were used to test for a new insertion in *CER1*, causing the mutant *cer1* sector in combination with the *I/dSpm* terminal inverted repeats primer (T; Figure 4). PCR conditions for primers 1 to 6 and T were 5 min at 94°C, followed by 30 cycles of 94°C (30 sec), 55°C (30 sec), and 72°C (3 min). In addition to the cDNA sequence, the sequence of a single strand of genomic DNA up to 1656 bp upstream of the *CER1* start codon was determined.

The cDNA sequence and the predicted amino acid sequence were analysed using the PC/Gene computer package (IntelliGenetics, Geneva, Switzerland).

Data Base Searches

GenBank and expressed sequence tag (EST) data bases were searched for *CER1* homologs using BLAST programs (Altschul et al., 1990). GenBank accession numbers of the reported homologous sequences are L33792 for the *Senecio odorus* SOLIPTRB partial cDNA; T22420 and Z18418 for two Arabidopsis ESTs with nearly 100% identity with the *CER1* cDNA; Z25487 for the Arabidopsis ATTS1001 EST; L35835 for the *Brassica campestris* EST; R27543 for the potato EST; T70657 for the maize EST; D15324 and D22308 for two rice ESTs with N-terminal homology with CER1; and D40658 and D23996 for two rice ESTs with internal homology. The cDNA clones corresponding to the four rice ESTs have been kindly obtained from Yoshiaki Nagamura of the Rice Genome Research Program (STAFF Institute, Ibaraki, Japan). The 5′ ends of both D15324 and D22308 have been resequenced to correct for frameshifts and other occasional misreadings found in the original data base sequence. The *CER1* cDNA sequence data and genomic DNA sequence data have been deposited in the EMBL, GenBank, and DDBJ data bases with accession numbers D64155 and D64156, respectively.

Microscopy

Germination of *cer1-m*, *cer1-1*, and wild-type pollen was examined by bright-field and fluorescent microscopy after staining with aniline blue according to Preuss et al. (1993). Revertant excision sectors and mutant insertion sectors on 4- to 5-week-old stems were examined with a preparation microscope. For a more detailed observation, fresh 1-cm-long stem parts were excised and mounted on stubs; the excision wounds were closed with rapidly drying cyano-acrylate glue. Subsequently, they were transferred to a scanning electron microscope (model No. 5200; JOEL Ltd., Tokyo, Japan), partially dehydrated for 5 min in the vacuum of this microscope, and finally photographed at 15 kV. Closing the wounds prevented excessive water loss from the specimens, which would have disturbed the vacuum of the microscope; the (gentle) dehydration step was introduced to better expose the epidermis cell boundaries.

For scanning and transmission electron microscopy of tryphine on pollen grains, freshly opened anthers were fixed in 3% glutaraldehyde in 0.7 M cacodylate buffer for 15 min, rinsed in the buffer several times, postfixed in 1% osmium tetroxide in the same buffer for 15 min, and stepwise dehydrated into ethanol 100%; all treatments were performed at room temperature. For scanning electron microscopy, specimens were critical point dried via carbon dioxide, mounted on stubs, coated with platinum, and observed in a JEOL 6300 field-emission scanning electron microscope at 5 kV. For transmission electron microscopy, the 100% ethanol–saturated specimens were stepwise infiltrated with resin (Spurr, 1969), polymerized, ultrathin sectioned, stained with lead citrate and uranyl acetate, and observed in a JEOL 1200 transmission electron microscope at 80 kV.

ACKNOWLEDGMENTS

We thank Maarten Koornneef for sharing his experience with *cer* mutants and for critically reading the manuscript. We thank Christiane Leonards-Schippers for helpful discussions, Jan-Peter Nap for reading the manuscript critically, and Gerrit Stunnenberg and Gerard Scholten for taking care of the plants in the greenhouse. We also thank the members of our European Scientists Sequencing Arabidopsis (ESSA) DNA sequencing team for their support in DNA sequencing and Bauke Ylstra for his advice on the analysis of pollen germination. Our colleagues at the DLO-Centrum voor Fotografie en Beeldverwerking are gratefully acknowledged for making the photographs of *cer1* and *CER1* sectors and for their help in preparing the other figures. This work was supported by the European Union BRIDGE/BIOTECH project (Grant No. BIOT-CT90-0207) on Development and Use of *Arabidopsis thaliana* as a Tool for Isolating Genes of Agronomic Importance.

Received July 12, 1995; accepted October 4, 1995.

REFERENCES

Aarts, M.G.M., Dirkse, W.G., Stiekema, W.J., and Pereira, A. (1993). Transposon tagging of a male sterility gene in *Arabidopsis*. Nature **363,** 715–717.

Aarts, M.G.M., Corzaan, P., Stiekema, W.J., and Pereira, A. (1995). A two-element *Enhancer-Inhibitor* transposon system in *Arabidopsis thaliana*. Mol. Gen. Genet. **247,** 555–564.

Altschul, S.F., Gish, W., Miller, W., Myers, E.W., and Lipman, D.J. (1990). Basic local alignment search tool. J. Mol. Biol. **215,** 403–410.

Arondel, V., Lemieux, B., Hwang, I., Gibson, S., Goodman, H.M., and Somerville, C.R. (1992). Map-based cloning of a gene controlling omega-3 fatty acid desaturation in Arabidopsis. Science **258,** 1353–1355.

Arthington, B.A., Bennet, L.G., Skatrud, P.L., Guynn, C.J., Barbuch, R.J., Ulbright, C.E., and Bard, M. (1991). Cloning, disruption and sequence of the gene encoding yeast C-5 sterol desaturase. Gene **102,** 39–44.

Baker, E.A. (1974). The influence of environment on leaf wax development in *Brassica oleracea* var. *gemmifera*. New Phytol. **73,** 955–966.

Bianchi, A., Bianchi, G., Avato, P., and Salamini, F. (1985). Biosynthetic pathways of epicuticular wax of maize as assessed by mutation, light, plant age and inhibitor studies. Maydica **30,** 179–198.

Cheesbrough, T.M., and Kolattukudy, P.E. (1984). Alkane biosynthesis by decarbonylation of aldehydes catalyzed by a particulate preparation from *Pisum sativum*. Proc. Natl. Acad. Sci. USA **81,** 6613–6617.

Dennis, M., and Kolattukudy, P.E. (1992). A cobalt-porphyrin enzyme converts a fatty aldehyde to a hydrocarbon and CO. Proc. Natl. Acad. Sci. USA **89,** 5306–5310.

Devereux, J., Haeberli, P., and Smithies, O. (1984). A comprehensive set of sequence analysis programs for the VAX. Nucleic Acids Res. **12,** 387–395.

Eigenbrode, S.D., and Espelie, K.E. (1995). Effects of plant epicuticular lipids on insect herbivores. Annu. Rev. Entomol. **40,** 171–194.

Goldberg, R.B., Beals, T.P., and Sanders, P.M. (1993). Anther development: Basic principles and practical applications. Plant Cell **5,** 1217–1229.

Hall, D.M., and Jones, R.L. (1961). Physiological significance of surface wax on leaves. Nature **191,** 95–96.

Hannoufa, A., McNevin, J., and Lemieux, B. (1993). Epicuticular waxes of *eceriferum* mutants of *Arabidopsis thaliana*. Phytochemistry **33,** 851–855.

Haque, M.M., Mackill, D.J., and Ingram, K.T. (1992). Inheritance of leaf epicuticular wax content in rice. Crop Sci. **32,** 865–868.

Iba, K., Gibson, S., Nishiuchi, T., Fuse, T., Nishimura, M., Arondel, V., Hugly, S., and Somerville, C. (1993). A gene encoding a chloroplast ω-3 fatty acid desaturase complements alterations in fatty acid desaturation and chloroplast copy number of the *fad7* mutant of *Arabidopsis thaliana*. J. Biol. Chem. **268,** 24099–24105.

Jenks, M.A., Tuttle, H.A., Eigenbrode, S.D., and Feldmann, K.A. (1995). Leaf epicuticular waxes of the *eceriferum* mutants in *Arabidopsis*. Plant Physiol. **108,** 369–377.

Kok, M., Oldenhuis, R., van der Linden, M.P.G., Raatjes, P., Kingma, J., van Lelyveld, P.H., and Witholt, B. (1989). The *Pseudomonas oleovorans* alkane hydroxylase gene. J. Biol. Chem. **264,** 5435–5441.

Kolattukudy, P.E. (1975). Biochemistry of cutin, suberin and waxes, the lipid barriers on plants. In Recent Advances in the Chemistry and Biochemistry of Plant Lipids, T. Galliard and E.I. Mercer, eds (New York: Academic Press), pp. 203–246.

Kolattukudy, P.E., ed (1976). Chemistry and Biochemistry of Natural Waxes. (Amsterdam: Elsevier).

Kolattukudy, P.E. (1980). Cutin, suberin and waxes. In The Biochemistry of Plants, Vol. 4, Lipids: Structure and Function, P.K. Stumpf, ed (New York: Academic Press), pp. 571–645.

Koornneef, M., Hanhart, C.J., and Thiel, F. (1989). A genetic and phenotypic description of *eceriferum* (*cer*) mutants in *Arabidopsis thaliana*. J. Hered. **80,** 118–122.

Lemieux, B., Koornneef, M., and Feldmann, K.A. (1994). Epicuticular wax and *eceriferum* mutants. In *Arabidopsis*, E.M. Meyerowitz and C.R. Somerville, eds (Cold Spring Harbor, NY: Cold Spring Harbor Laboratory Press), pp. 1031–1047.

Masson, P., Strem, M., and Fedoroff, N. (1991). The *tnpA* and *tnpD* gene products of the *Spm* element are required for transposition in tobacco. Plant Cell **3,** 73–85.

McNevin, J.P., Woodward, W., Hannoufa, A., Feldmann, K.A., and Lemieux, B. (1993). Isolation and characterization of *eceriferum* (*cer*) mutants induced by T-DNA insertions in *Arabidopsis thaliana*. Genome **36,** 610–618.

Newman, T., de Bruijn, F.J., Green, P., Keegstra, K., Kende, H., McIntosh, L., Ohlrogge, J., Raikhel, N., Somerville, S., Thomashow, M., Retzel, E., and Somerville, C. (1994). Genes galore: A summary of methods for accessing results from large-scale partial sequencing of anonymous *Arabidopsis* cDNA clones. Plant Physiol. **106,** 1241–1255.

Okuley, J., Lightner, J., Feldmann, K., Yadav, N., Lark, E., and Browse, J. (1994). Arabidopsis *FAD2* gene encodes the enzyme that is essential for polyunsaturated lipid synthesis. Plant Cell **6,** 147–158.

O'Toole, J.C., and Cruz, R.T. (1983). Genotypic variation in epicuticular wax of rice. Crop Sci. **23,** 392–394.

Podila, G.K., Rogers, L.M., and Kolattukudy, P.E. (1993). Chemical signals from avocado surface wax trigger germination and appressorium formation in *Colletotrichum gloeosporioides*. Plant Physiol. **103,** 267–272.

Preuss, D., Lemieux, B., Yen, G., and Davis, R.W. (1993). A conditional sterile mutation eliminates surface components from *Arabidopsis* pollen and disrupts cell signaling during fertilization. Genes Dev. **7,** 974–985.

Pyee, J., Hongshi, Y., and Kolattukudy, P.E. (1994). Identification of a lipid transfer protein as the major protein in the surface wax of broccoli (*Brassica oleracea*) leaves. Arch. Biochem. Biophys. **311,** 460–468.

Reddy, A.S., Nuccio, M.L., Gross, L.M., and Thomas, T.L. (1993). Isolation of a Δ6-desaturase gene from the cyanobacterium *Synechocystis* sp. strain PCC6803 by gain-of-function expression in *Anabaena* sp. strain PCC7120. Plant Mol. Biol. **27,** 293–300.

Sakamoto, T., Wada, H., Nishida, I., Ohmori, M., and Murata, N. (1994). Identification of conserved domains in the Δ12 desaturases of cyanobacteria. Plant Mol. Biol. **24,** 643–650.

Shanklin, J., White, E., and Fox, B.G. (1994). Eight histidine residues are catalytically essential in a membrane-associated iron enzyme, stearoyl-CoA desaturase, and are conserved in alkane hydroxylase and xylene monooxygenase. Biochemistry **33,** 12787–12794.

Spurr, A.R. (1969). A low viscosity epoxy resin embedding medium for electron microscopy. J. Ultrastruct. Res. **71,** 173–184.

Städler, E. (1986). Oviposition and feeding stimuli in leaf surface waxes. In Insects and the Plant Surface, B. Juniper and R. Southwood, eds (London: Edward Arnold), pp. 105–121.

Sterk, P., Booij, H., Schellekens, G.A., Van Kammen, A., and De Vries, S.C. (1991). Cell-specific expression of the carrot EP2 lipid transfer protein gene. Plant Cell **3,** 907–921.

Stukey, J.E., McDonough, V.M., and Martin, C.E. (1990). The *OLE1* gene of *Saccharomyces cerevisiae* encodes the Δ9 fatty acid desaturase and can be functionally replaced by the rat stearoyl-CoA desaturase gene. J. Biol. Chem. **265,** 20144–20149.

Suzuki, M., Hayakawa, T., Shaw, J.P., Rekik, M., and Harayama, S. (1991). Primary structure of xylene monooxygenase: Similarities to and differences from the alkane hydroxylation system. J. Bacteriol. **173,** 1690–1695.

Thiede, M.A., Ozols, J., and Strittmatter, P. (1986). Construction and sequence of cDNA for rat liver stearyl coenzyme A desaturase. J. Biol. Chem. **261,** 13230–13235.

Thoma, S., Kaneko, Y., and Somerville, C. (1993). A non-specific lipid transfer protein from *Arabidopsis* is a cell wall protein. Plant J. **3,** 427–436.

Thoma, S., Hecht, U., Kippers, A., Botella, J., de Vries, S., and Somerville, C. (1994). Tissue-specific expression of a gene encoding a cell wall–localized lipid transfer protein from *Arabidopsis*. Plant Physiol. **105,** 35–45.

Thompson, K.F. (1963). Resistance to the cabbage aphid (*Brevicoryne brassicae*) in Brassica plants. Nature **198,** 209.

von Wettstein-Knowles, P. (1979). Genetics and biosynthesis of plant epicuticular waxes. In Advances in the Biochemistry and Physiology of Plant Lipids, L.-Å. Appelqvist and C. Liljenberg, eds (Amsterdam: Elsevier/North-Holland Biomedical Press), pp. 1–26.

von Wettstein-Knowles, P. (1994). Biosynthesis and genetics of waxes. In Waxes: Chemistry, Molecular Biology and Functions, R.J. Hamilton, ed (Dundee, UK: Oily Press), pp. 91–129.

Wada, H., Gombos, Z., and Murata, N. (1990). Enhancement of chilling tolerance of a cyanobacterium by genetic manipulation of fatty acid desaturation. Nature **347,** 200–203.

Woodhead, S., and Padgham, D.E. (1988). The effect of plant surface characteristics on resistance of rice to the brown planthopper, *Nilaparvata lugens*. Entomol. Exp. Appl. **47,** 15–22.